

Intramolecular FRET Efficiency Measures for Time-Lapse Fluorescence Microscopy Images

Mark Holden^(✉)

Graduate School of Informatics, Kyoto University, Kyoto, Japan
mark_holden@i.kyoto-u.ac.jp

Abstract. Here we investigate quantitative measures of Förster resonance energy transfer (FRET) efficiency that can be used to quantify protein-protein interactions using fluorescence microscopy images of living cells. We adopt a joint intensity space approach and develop a parametric shot noise model to estimate the uncertainty of FRET efficiency on a per pixel basis. We evaluate our metrics rigorously by simulating photon emission events corresponding to typical conditions and demonstrate advantages of our metrics over the conventional ratiometric one. In particular, our measure is linear, normalised and has greater tolerance to low SNR characteristic of FRET fluorescence microscopy images.

1 Introduction

The understanding of cellular processes is at the frontier of bio-medical research [11]. The conventional optical microscope has been the key observational instrument for microbiology for centuries, however its resolution is diffraction limited to around 200 nm, whereas many cellular processes occur at molecular scales of just a few nm. This limitation has recently motivated several decades of research on imaging methods able to detect objects smaller than the optical diffraction limit. One of the most successful approaches is fluorescence microscopy which makes use of fluorophores (fluorescent proteins) that were originally discovered in the jellyfish *Aequorea victoria* by Shimomura *et al.* [15]. Fluorophores can be excited with a narrow band of photons and emit photons of similar wavelengths. They can be bound to biologically active molecules and used to probe the dynamics of many molecular processes in living organisms. Many fluorescence microscopy methods have emerged to determine fluorophore motion, see the recent review [8]. A widely used one is known as Förster resonance energy transfer (FRET) [5]. FRET has several advantages compared with other methods: (a) it can detect fluorophore separation distances of just a few nm, ideal for studying sub-cellular molecular processes; (b) it can be targeted to specific protein-protein interactions; (c) it can be applied *in-vivo*. FRET imaging is based on a pair of fluorophores that interact by electric dipole-dipole coupling. The efficiency of this dipole interaction, denoted $E(r)$ where r is the separation distance, was found by Förster [5] to be $E(r) = \frac{1}{1 + \frac{r^6}{r_0^6}}$ where r_0 is known as the Förster distance. Because of the rapid decrease in efficiency with r dipoles only

interact significantly when $r \approx r_0$, which typically corresponds to $r < 10$ nm. The fluorophore pair is chosen so that the two fluorophores are excited by, and emit, photons of slightly different frequencies so that filters can be applied to separate the two signals. When energy is transferred during this interaction one fluorophore (donor) loses energy while the other (acceptor) gains energy. This results in a corresponding decrease in donor, and increase in acceptor emission. Recently there have been several advances in fluorescence microscopy hardware which has led to its increasing use by bio-medical researchers. Despite these advances many researchers assess images qualitatively. Quantitative image processing methods are potentially of enormous benefit. However, conventional methods often do not perform well. For instance, a recent evaluation study of methods to detect isolated fluorophores [16] found that the performance of state-of-the-art object detection methods was significantly compromised due to the low SNR. This is because the relatively small number of fluorescent molecules result in a much smaller number of photons detected for fluorescence images when compared to typical optical images. Typically, as few as ten fluorescent photons are detected per pixel. As a consequence, fluorescent microscopy images are characterized by Poisson, rather than Gaussian, distributed noise (shot noise) and have low SNR. Furthermore, many biological researchers are interested in dynamical processes and use time-lapse microscopy which decreases exposure time and leads to very low SNR, typically in the range 2 to 3.

There are three main imaging methods for measuring E : intensity based FRET, Fluorescence lifetime and anisotropy imaging, see [9, 19]. Fluorescence lifetime methods rely on fluorescence-decay histograms to accurately fit decay curves. This requires a relatively greater number of photons and so reduces spatio-temporal resolution. Anisotropy methods rely on polarization which reduces the number of photons collected. The advantages and disadvantages of these imaging methods for the living cell is discussed in [13]. In summary, intensity based FRET is used in most laboratories [19]. The standard method of measuring FRET for intensity based images is to calculate the ratio of the acceptor:donor intensity, see [9]. However, this has the disadvantage of not being linear in E . Linearity can be achieved by using the donor only FRET signal as proposed by Birtwistle *et al.* [2]. Image noise impacts the measurement of E , however, there is very little existing work in this area. Recently we introduced a measure of E for FRET imaging in general [7] that is linear and has the advantage of using both donor and acceptor FRET signals. Here we extend this work and specifically focus on measuring E using intra-molecular FRET biosensors with a fixed one-one stoichiometry. We establish a quantitative imaging model and derive the $(1 - E)^{-1}$ dependence of the standard ratio measure based on Gordon *et al.* [6]. We investigate the accuracy of a Poisson noise model and use this to derive a new fractional uncertainty FRET measure. We test the measures by simulation of photon emission with shot noise and demonstrate that our measures are unbiased. Finally we apply our measures to real-world clinical atherosclerosis data and demonstrate structure consistent with biological expectation.

2 Quantitative FRET Imaging Model

Intramolecular FRET biosensors are designed to target particular proteins within a molecular pathway to measure the level of activation of that pathway. The biosensor is typically genetically encoded and is expressed by every targeted cell. Figure 1 shows a schematic illustration of the architecture of an intramolecular FRET biosensor designed to measure EGF signalling. There are several similar architectures, see [1] for further details. The key component is a pair of fluorophores which fluoresce at slightly different wavelengths and interact through electric dipole coupling (FRET). These fluorophores are attached to specific proteins in the pathway and the conformational change causes a change in the separation distance r that can be detected by FRET. In the example of Fig. 1, the donor and acceptor are attached to SH3 (sensor) and SH2 (ligand) protein sub-domains respectively. When an epidermal growth factor (EGF) signalling molecule binds to its receptor (EGFR) it induces the phosphorylation of CrkII on tyrosine 221, which produces a residue that binds to SH2 [14]. As a consequence the protein complex changes from an open to a closed conformational state. The donor and acceptor fluorophores are continuously excited by photons at rates γ_d^* and γ_a^* (not shown) and emit photons at rates γ_d and γ_a . In the open state, shown left, r is much greater than the Förster distance r_0 , a few nm , and their electric dipoles do not interact. In the closed state, shown right, $r \approx r_0$ and so their dipoles interact and energy is transferred from donor to acceptor. This results in a decrease in the donor, and an increase in the acceptor photon emission rates γ_d and γ_a . So, in summary, the donor and acceptor fluorophores emit photons at rates γ_{d0} , γ_{a0} when $r \gg r_0$ and at rates γ_{d1} , γ_{a1} when $r \lesssim r_0$. The photons emitted by the donor and acceptor fluorophores are filtered into two channels and converted by the microscope into two electrical signals. These signals are amplified independently and sampled to produce two digital images, one for the set of donor I_d fluorophores and one for the set of acceptor I_a . The pixel intensity, for a fluorophore image, I , is linearly related to the number of photons detected for that pixel, γ such that: $I = \alpha\gamma$. Here α denotes the gain factor which depends on how the photon signal is filtered, amplified and sampled to a pixel intensity. Accordingly, when the fluorophore separation distance r is such that $r \gg r_0$, the fluorophores do not interact and since their relative concentration is fixed the donor and acceptor image intensities I_d and I_a are linearly related, as follows:

$$I_{a0} = g_0 I_{d0} \quad (1)$$

where the zero subscript denotes negligible dipole interaction (no FRET). The constant of proportionality g_0 is related to the efficiency of the fluorophores and the gains α_d and α_a . When r decreases so that $r \lesssim r_0$ energy is transferred from the donor to acceptor fluorophore. Hence I_d decreases while I_a increases, so the change in intensities $\Delta I_d(r)$ and $\Delta I_a(r)$ can be written as:

$$\begin{aligned} \Delta I_d(r) &= I_{d0} - I_{d1}(r) \geq 0 \\ \Delta I_a(r) &= I_{a1}(r) - I_{a0} \geq 0 \end{aligned} \quad (2)$$

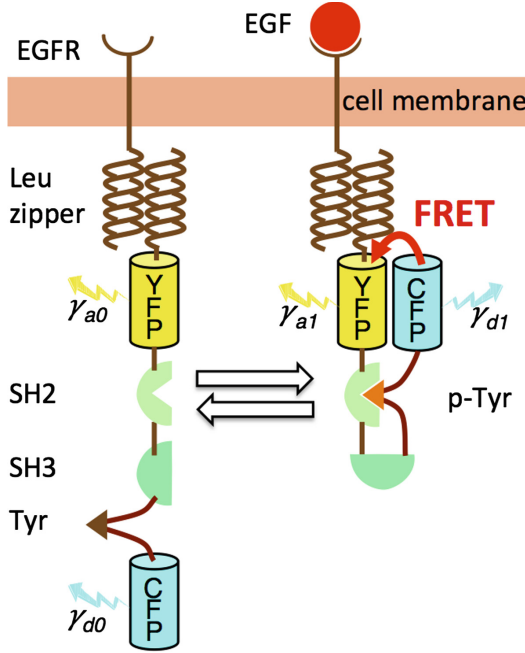


Fig. 1. Schematic illustration of imaging method with a intramolecular FRET biosensor. Two fluorophores, donor (CFP) and acceptor (YFP), are attached to the SH2 and SH3 protein domains. When epidermal growth factor (EGF) binds to the receptor (EGFR) it stimulates Tyrosine (Tyr) phosphorylation (p-Tyr) which binds to the SH2 protein domain. This causes a conformational change in the protein complex which reduces the donor-acceptor separation distance that is detected by FRET.

Here the subscript one denotes dipole interaction and zero denotes no interaction. In [6] the changes in intensity associated with the dipole interaction are related linearly to $E(r)$ and the free donor intensity I_{d0} as follows:

$$\left. \begin{aligned} \Delta I_d(r) &= E(r)I_{d0} \\ \Delta I_a(r) &= g_1 E(r)I_{d0} \end{aligned} \right\} \Rightarrow \frac{\Delta I_a}{\Delta I_d} = g_1 \quad (3)$$

Here the constant of proportionality denoted by g_1 , G in [6], depends on the ratio of the quantum yields, $\frac{\text{\#photons emitted}}{\text{\#photons absorbed}}$, of the donor and acceptor fluorophores and the filter efficiencies [6]. So the fluorophore image intensities I_d , I_a are related by two linear Eqs. (2) and (3). In summary, Gordon *et al.* [6] provide a imaging model where changes fluorophore image intensities are linearly related to E , but the model ignores: (a) image noise; (b) diffraction effects; (c) inhomogeneous FRET states within a single pixel.

3 Measuring FRET Efficiency

First we analyse the standard ratio metric $\frac{I_a}{I_d}$. Its dependence on the efficiency $E(r)$ can be derived from Eqs. (1), (2), (3) as follows:

$$\begin{aligned} \frac{I_{a1}}{I_{d1}} &= \frac{I_{a0} + g_1 I_{d0} E}{(1 - E) I_{d0}} \\ &= \frac{g_0 + g_1 E}{(1 - E)} \\ &= \frac{g_0 + g_1}{(1 - E)} - g_1 \end{aligned} \quad (4)$$

Equation (4) indicates that it is linear in $(1 - E)^{-1}$. Figure 2 shows a plot of the relationship. Since the photons emitted by biosensors within a pixel add linearly we require a measure that preserves this property. We argue that a non-linear measure cannot achieve this and so is unsuitable as a quantitative measure of FRET efficiency. Therefore we require to determine a more suitable one.

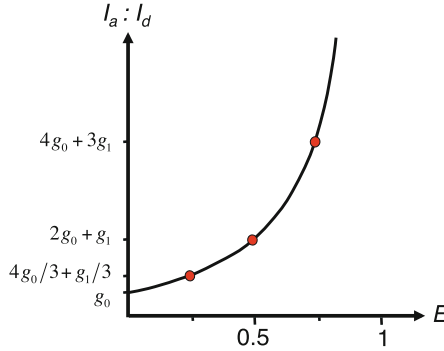


Fig. 2. Non-linear relationship between the intensity ratio $\frac{I_a}{I_d}$ and E .

We can gain insight into the problem by placing the imaging model equations in the joint donor and acceptor intensity space $I_d \times I_a$ as shown in Fig. 3. We can see that the two linear equations are represented by the blue line, $I_a = g_0 I_d$, and the red line, corresponding to the intensity transition due to FRET. The position on the blue line $I_a = g_0 I_d$ depends on the concentration of fluorophores. The greater the concentration, the more photons are emitted so the larger are both I_d and I_a . The length of the red line depends on the amount of energy transferred or efficiency of FRET. We therefore propose that the length of the red line is a 'natural' measure of the amount of FRET. This length is just the Euclidean norm of intensity change ΔI_d and ΔI_a . Since both ΔI_d and ΔI_a are

linear in E by Eq. (3) then so is the Euclidean norm d_f , which we refer to as JIN (Joint Intensity Norm), we can write:

$$\begin{aligned} d_f &= \sqrt{\Delta I_d^2 + \Delta I_a^2} \\ &= \sqrt{1 + g_1^2} E(r) I_{d0} \end{aligned} \quad (5)$$

It is straightforward to determine the normalised measure d_{fn} . Simply by dividing the maximal value of d_f , $d_f(E = 1) = \sqrt{1 + g_1^2} I_{d0}$. This is the length of the g_1 line from the intercept with the y -axis, $I_d = 0$, corresponding to $E = 1$, to (I_{d0}, I_{d0}) . This gives $d_{fn} = \frac{d_f}{(\sqrt{1 + g_1^2}) I_{d0}}$.

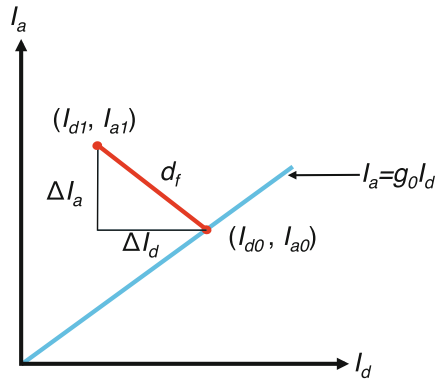


Fig. 3. Donor and acceptor intensities with and without FRET. When there is no dipole interaction (no FRET) I_a and I_d are linearly dependent on the intra-pixel biosensor concentration, shown by the blue line. When dipoles interact FRET occurs and there is a transition from a point on this blue line (I_{d0}, I_{a0}) in the direction g_1 to the point (I_{d1}, I_{a1}) , shown by the red line. The length of the red line d_f is a linear measure of the FRET efficiency. (Color figure online)

4 Uncertainty of FRET Efficiency Measure

We aim to determine a quantitative noise model and use it to predict the uncertainty of our measure of FRET efficiency. First we recognize that fluorescence photons are emitted randomly as probabilistic quantum events. These events constitute a counting experiment and so conform to Poisson statistics. Because of the small photon count, photomultipliers are often the preferred detectors. A photomultiplier is a multi-stage amplifier. The first stage, photocathode, converts photons into electrons by the photoelectric effect. The second and subsequent stages, dynodes, amplify the electrons by secondary emission. Both of these stages involve quantum mechanical processes which have Poisson statistics. A photomultiplier can be considered as a cascade of Poisson processes which is

itself a Poisson process [4]. If solid state devices are used then they are likely to contribute to signal independent Gaussian distributed noise. Hence, in general, the observed signal I has two components, a signal dependent Poisson noise component Q and signal independent Gaussian noise component W , s.t. $I = \alpha Q + W$ where α is the gain, see [10]. Q and W can be modelled as random variables. Q has a single parameter, emission rate, λ discrete Poisson probability density function given by: $P(y = x|\lambda) = \frac{e^{-\lambda} \lambda^x}{x!}$, where $x \in \mathbb{N}_0$. Note that for a Poisson random variable y , the mean \bar{y} equals the variance $\sigma^2(y)$ and the uncertainty of y equals its standard deviation so $\delta y = \sigma(y) = \sqrt{\bar{y}}$, see [17] Chap. 11. W has a normal probability density function given by: $P(x|\mu, \sigma^2) = \frac{1}{\sqrt{2\pi\sigma^2}} e^{-\frac{(\mu-x)^2}{2\sigma^2}}$ where μ is the mean and σ^2 the variance. The shot noise component Q can be reduced by increasing the photon count while the noise component W can be reduced by using low noise components or by cooling. We investigated the noise characteristics of our microscope images experimentally. We used time lapse images and manually defined two rectangular ROIs for each of the donor and acceptor image sequences. One ROI for background samples, uniform minimal intensity, the other in the foreground samples, uniform maximal intensity, likely to correspond to FRET events. We selected a series of frames for which the signal was uniform so that we had over 10^5 intensity samples. Then we compensated for amplifier gain and fitted a Poisson distribution to the rescaled signal using `poissfit` (matlab, Mathworks, MA, USA). The results are shown in Fig. 4. These clearly show that the distributions for both ROIs, for both (a) donor and (b) acceptor, can be accurately modelled as Poisson distributions. This result suggests that noise (uncertainty) is predominantly shot noise and the signal independent Gaussian component is a lot smaller. Hence for our time lapse sequence we use a pure shot noise model and neglect the signal independent W term. We make use of this result and use a shot noise model to estimate the uncertainty of d_f in Fig. 3. d_f is a distance between two joint intensity samples (I_{d0}, I_{a0}) and

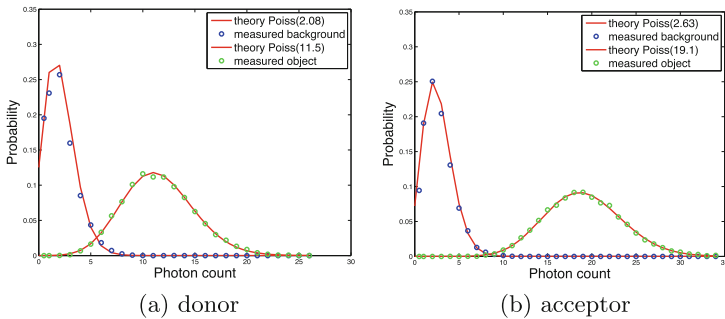


Fig. 4. Poisson fit to rescaled pixel intensities of background (blue circles) and foreground (green circles). (a) donor image, (b) acceptor image. The best fits are shown as solid red curves. The means of the distributions is given in the legends. (Color figure online)

(I_{d1}, I_{a1}) in the direction g_1 . The samples (I_{d0}, I_{a0}) lie on the g_0 line which can be determined precisely since we have many samples of this, so we may ignore its uncertainty and we need only consider the point (I_{d1}, I_{a1}) . In the joint intensity space noise can be represented as an uncertainty ellipse where the axes correspond to the uncertainty of the donor and acceptor intensity which we denote as σ_d and σ_a . We need a scalar value of uncertainty which we refer to as σ_f , this can be obtained by projecting this uncertainty ellipse onto the red line. By geometrical argument $\sigma_f = \sqrt{\frac{1+g_1^2}{\frac{1}{\sigma_d^2} + \frac{g_1^2}{\sigma_a^2}}}$. Now we need obtain estimates for σ_d and σ_a .

Since photon emission is a Poisson process, its uncertainty σ is the square root of the mean photon count rate. Furthermore, since pixel intensity is the mean count rate multiplied by the gain α , the fractional uncertainty of intensity equals that of the photon count, [17] page 54. Hence we may estimate the uncertainty of intensity σ_I in terms of the mean intensity and gain as follows: $\sigma_I = \sqrt{\alpha I}$. We therefore can predict the uncertainty of d_f . To determine a fractional uncertainty d_{fu} we divide this uncertainty by the best estimate of d_f which gives: $d_{fu} = \frac{\sigma_f}{d_f}$.

5 Evaluation

We have developed d_f , a measure of E , and d_{fu} an estimate of the fractional uncertainty of d_f . In this section we evaluate the accuracy of these measures and compare them with the standard one. Ideally we would have ground truth FRET images with known separation distances and uncertainties. However, it is very difficult and costly to produce such data. So instead, our evaluation strategy is based on simulation of the photon emission events corresponding to realistic FRET experiments which gives quantitative results, and qualitative evaluation of results for clinical images. We argue that this is a robust evaluation strategy.

Implementation

There are four important parameters needed to determine d_f , d_{fn} and d_{fu} , namely: g_0 , g_1 , α_d , α_a . If we assume shot noise then g_0 , α_d and α_a can be estimated from the mean and variance of intensity sample in a ROI. The g_1 parameter is probably the most difficult one to estimate. Because it is needed to compare results across different platforms there are a number of existing imaging methods. For example, Zal and Gascoigne [18] estimate g_1 using donor recovery after acceptor photobleaching. Our implementation provides a pixelwise measure of d_f etc. Given an input intensity sample (I_d, I_a) it first determines whether the sample lies in a valid half space, compared to $I_a = g_0 I_d$. Then it finds the point of intersection (I_{d0}, I_{a0}) with the line $I_a = g_0 I_d$ and determines d_f by calculating the Euclidean norm. The intercept $(0, I_a)$ of the g_1 line is used to determine d_{fn} . The uncertainty of the sample (I_{d1}, I_{a1}) is estimated using the gain and intensity value and the projected uncertainty σ_f is calculated from the equation derived in the previous section which gives d_{fu} .

Accuracy

We estimated the accuracy of the proposed measures d_f , d_{fn} and d_{fu} as a function of the FRET efficiency $E(r)$ and SNR and included the standard $\frac{I_a}{I_d}$ ratio measure for comparison. To assess the measures quantitatively we developed a strategy of modeling the photon count γ as a Poisson distributed random variable using the imnoise function of Matlab. We used four independent random variables to generate: γ_{d0} , γ_{a0} , γ_{d1} and γ_{a1} . We used realistic values for these and α_d , α_a and g_1 based on the experimental results. We assumed linear signal amplification and the free donor Eq. (1) to calculate I_{d0} and I_{a0} . The intensities I_{d1} and I_{a1} are functions of the FRET efficiency E . We calculate these using the FRET efficiency Eqs. (2) and (3). We varied E over the range 0 to 0.8 in 0.01 steps. For each value of E , we generated 100 instances of the photon count random variables γ_{d0} , γ_{a0} , γ_{d1} and γ_{a1} and used these to generate the intensities I_{d0} , I_{a0} , I_{d1} , I_{a1} and the FRET measures d_f , d_{fu} and ratio for each instance. Figure 5 shows the average values, of 100 instances, of d_f , d_{fu} and $\frac{I_a}{I_d}$. The theoretical model is also shown to assess bias. Figure 5 (a) and (b) indicate that d_f is a linear measure of $E(r)$ while $\frac{I_a}{I_d}$ is not. The accuracy of the model was

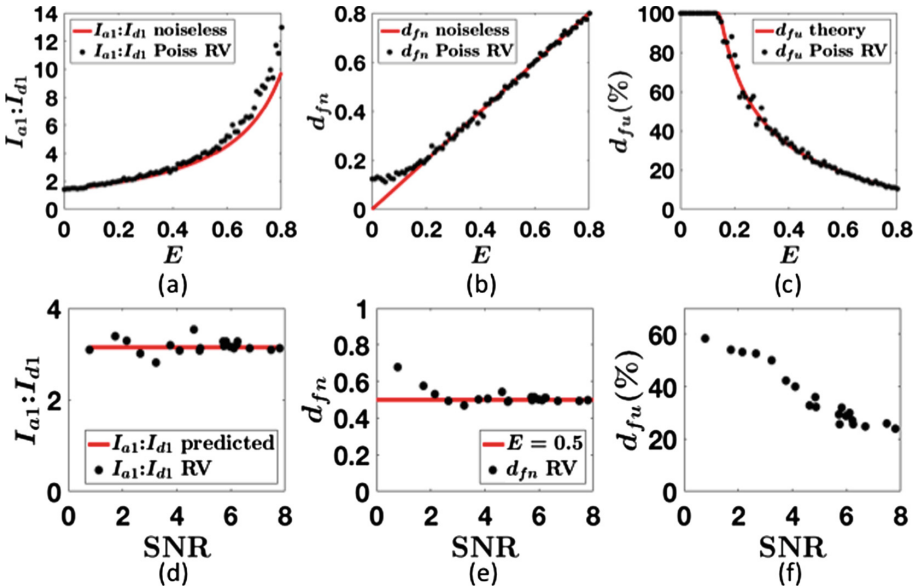


Fig. 5. (a)-(c) $\frac{I_a}{I_d}$, d_{fn} , d_{fu} FRET efficiency measures as a function of E . (a) The standard $\frac{I_a}{I_d}$ ratio measure predicted (red) and mean value for random variable (black). (b) d_{fn} normalised FRET measure theoretical (red) and mean value for random variable (black). (c) d_{fu} fractional uncertainty estimate theory (red) and median value for random variable (black), values clipped at 100%. (d)-(f) $\frac{I_a}{I_d}$, d_{fn} , d_{fu} measures respectively as a function of SNR with $E = 0.5$ with the true values in red. (Color figure online)

assessed by taking the theoretical model as ground truth x_{true} and calculating the fractional error: $\frac{\sigma(x-x_{true})}{|\bar{x}_{true}|}$. The fractional error for d_{fn} was 0.29 which is comparable to 0.25 for I_{d1} and 0.11 for I_{a1} , i.e. the noise level. The difference between the d_{fn} and the theoretical model in the region $E < 0.2$ is thought to be because of the non-symmetry of the Poisson distribution. Figure 5 (c) shows the median value of d_{fu} as a function of E . We used the median, because the mean was affected by outliers for low E . Values greater than 100% have been clipped to facilitate presentation. Figure 5 (d)-(f) are plots of (d) ratio, d_{fn} and (b) d_{fu} measures as a function of SNR for $E = 0.5$ solid line (red). The corresponding mean fractional error, over the SNR range, for d_{fn} and the ratio were 0.38 and 0.51 respectively, indicating that d_{fn} is more robust over typical SNR levels compared to the ratio measure. Figure 5 (f) shows the d_{fu} correlates highly with decreasing SNR, correlation coefficient $r = -0.95$.

Application to clinical images

We used a FRET timelapse sequence from a clinical atherosclerosis study which applied extracellular-signal-regulated kinase (ERK) FRET biosensors to detect signalling during thrombus formation. These images had very low SNR, between 2.4 and 3.1. Furthermore the joint intensity distribution in high signal regions was highly dispersed. We decided to address this using the denoising algorithm of Luisier [12] because of its capability of reducing mixed noise. Although, for this

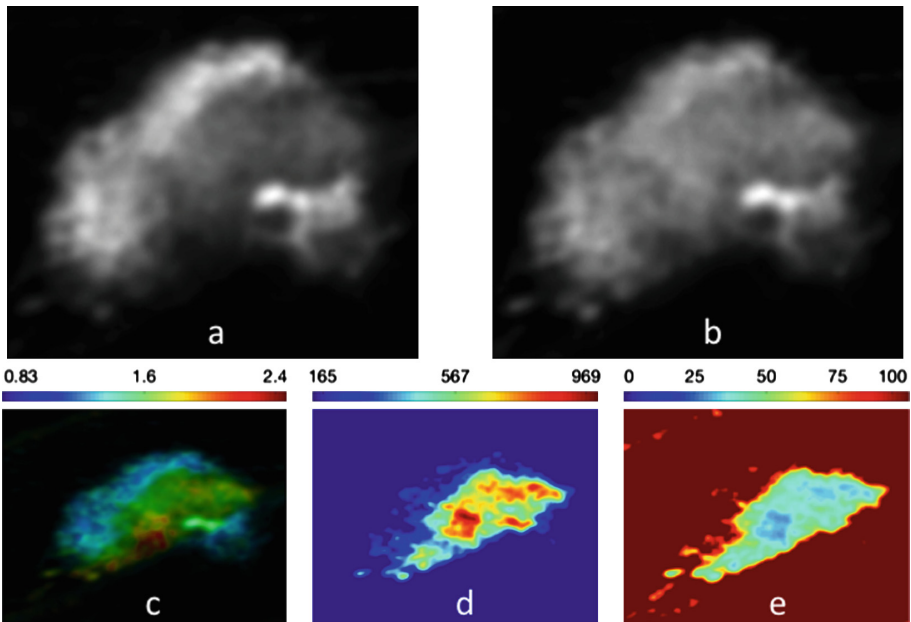


Fig. 6. FRET image pair and measures of E : (a) I_d , (b) I_a , (c) $\frac{I_a}{I_d}$, (d) d_f , (e) d_{fu} (%).

data we could have used a Poisson denoiser such as [3]. Any bias in the denoiser would lead to systematic error in our measures so we tested it thoroughly on a high signal region and noted: a large reduction in dispersion; small changes in local mean ($< 2\%$) and in the shape of the PDF; a doubling of SNR and no obvious artifacts. Figure 6 (a) and (b) show a donor (CFP) and acceptor (YFP) image frame during FRET. Note the lower intensity of the central part of the donor image. Figure 6 (c) shows the ratio image in intensity-modulated display IMD format. For IMD the ratio is linearly mapped to colour space and $\frac{I_a+I_d}{2}$ is mapped to gray scale. The colorbar indicates the upper and lower limits and values less than the lower limit are shown as black. Figure 6 (d) shows d_f and (e) shows d_{fu} fractional uncertainty. Signalling is thought to occur uniformly throughout the body of platelets so FRET efficiency should reflect their shape. During thrombosis platelets change shape and become blob or roughly hemispherical shaped with extruding filapods. We can see that the structure in (d) better matches this than in (c), indicating that d_f is more sensitive to FRET. Furthermore, the regions of lower uncertainty Fig. 6 (e) correspond to those more likely to be involved in thrombus formation, demonstrating the plausibility of our d_{fu} uncertainty estimate.

6 Conclusion

We have approached the problem of FRET measurement from the perspective of the joint intensity space and used the fundamental equations of FRET imaging to derive a linear measure of FRET d_f , in contrast to the standard ratio metric which has a $(1 - E)^{-1}$ dependence. We have demonstrated experimentally that the intensity distributions for our fluorescence microscopy images are consistent with a Poisson distributed shot noise model. We have used this to quantitatively model the intensity uncertainty with Poisson distributed random variables in the joint intensity space. We have combined this uncertainty measure with the FRET measure d_f to construct a new measure of the fractional uncertainty of FRET events d_{fu} . We have evaluated our measures by simulating the photon emission during FRET events as Poisson distributed random variables and real-world data. Our results have demonstrated: the linearity of our JIN d_f measure; that d_f is unbiased under typical noise conditions, and that the error in d_f is comparable to the intrinsic photon noise level. When applied to real-world data our d_f measure appears to produce image structure that is more consistent with biological expectation. Furthermore, the d_{fu} measure predicts the lowest uncertainty in regions thought likely to have signalling events during thrombosis.

Acknowledgements. Supported by Platform for Dynamic Approaches to Living Systems from MEXT Japan.

References

1. Aoki, K., Kiyokawa, E., Nakamura, T., Matsuda, M.: Visualization of growth signal transduction cascades in living cells with genetically encoded probes based on Förster resonance energy transfer. *Philos. Trans. R. Soc. Lond. B. Biol. Sci.* **363**(1500), 2143–2151 (2008)

2. Birtwistle, M.R., von Kriegsheim, A., Kida, K., Schwarz, J.P., Anderson, K.I., Kolch, W.: Linear approaches to intramolecular Förster resonance energy transfer probe measurements for quantitative modeling. *PloS one* **6**(11), e27823 (2011)
3. Boulanger, J., Kervrann, C., Bouthemy, P., Elbau, P., Sibarita, J.B., Salamero, J.: Patch-based nonlocal functional for denoising fluorescence microscopy image sequences. *IEEE Trans. Med. Imag.* **29**(2), 442–454 (2010)
4. Foord, R., Jones, R., Oliver, C.J., Pike, E.D.: The use of photomultiplier tubes for photon counting. *Appl. Opt.* **8**(10), 1975–1989 (1969)
5. Förster, T.: Intermolecular energy migration and fluorescence. *Ann. Phys.* **2**, 55–75 (1948)
6. Gordon, G.W., Berry, G., Liang, X.H., Levine, B., Herman, B.: Quantitative fluorescence resonance energy transfer measurements using fluorescence microscopy. *Biophys. J.* **74**, 2702–2713 (1998)
7. Holden, M.: A linear measure of Förster resonant energy transfer (FRET) efficiency incorporating a shot noise uncertainty model for fluorescence microscopy intensity images. In: *Proceedings of 13th IEEE International Symposium on Biomedical Imaging (ISBI)*, pp. 672–675. IEEE (2016)
8. Ishikawa-Ankerhold, H.C., Ankerhold, R., Drummen, G.P.C.: Advanced fluorescence microscopy techniques FRAP, FLIP, FLAP, FRET and FLIM. *Molecules* **17**(4), 4047–4132 (2012)
9. Jares-Erijman, E.A., Jovin, T.M.: FRET imaging. *Nat. Biotechnol.* **21**(11), 1387–1395 (2003)
10. Jezierska, A., Talbot, H., Chaux, C., Pesquet, J.C., Engler, G.: Poisson-Gaussian noise parameter estimation in fluorescence microscopy imaging. In: *Proceedings of 9th IEEE International Symposium on Biomedical Imaging (ISBI)*, pp. 1663–1666. IEEE (2012)
11. Lodish, H., Berk, A., Kaiser, C.A., Krieger, M., Bretscher, A., Ploegh, H., Amon, A., Scott, M.P.: *Molecular Cell Biology*. Freeman W. H., New York (2012)
12. Luisier, F., Blu, T., Unser, M.: Image denoising in mixed poisson-gaussian noise. *IEEE Trans. Image Process.* **20**(3), 696–708 (2011)
13. Padilla-Parra, S., Tramier, M.: FRET microscopy in the living cell: Different approaches, strengths and weaknesses. *BioEssays* **34**(5), 369–376 (2012)
14. Rosen, M.K., Yamazaki, T., Gish, G.D., Kay, C.M., Pawson, T., Kay, L.E.: Direct demonstration of an intramolecular sh2-phosphotyrosine interaction in the crk protein. *Nature* **374**, 477–479 (1995)
15. Shimomura, O., Johnson, F.H., Saiga, Y.: Extraction, purification and properties of aequorin, a bioluminescent protein from the luminous hydromedusan, aequorea. *J. Cell. Comput. Physiol.* **59**, 223–239 (1962)
16. Smal, I., Loog, M., Niessen, W., Meijering, E.: Quantitative comparison of spot detection methods in fluorescence microscopy. *IEEE Trans. Med. Imaging* **29**(2), 282–301 (2010)
17. Taylor, J.R.: *An Introduction to Error Analysis*. University Science Books, Herndon (1997)
18. Zal, T., Gascoigne, N.R.J.: Photobleaching-corrected FRET efficiency imaging of live cells. *Biophys. J.* **86**(6), 3923–3939 (2004)
19. Zeug, A., Woehler, A., Neher, E., Ponimaskin, E.G.: Quantitative intensity-based FRET approaches a comparative snapshot. *Biophys. J.* **103**(9), 1821–1827 (2012)